NETWORKED2A, an actin-membrane adaptor, binds specific protein kinases at the pollen tube plasma membrane.

Actin-Membrane Interactions Mediated by NETWORKED2 in Arabidopsis Pollen Tubes Through Associations with Pollen Receptor-Like Kinase 4 & 5.

Patrick Duckney[1*], Michael J. Deeks[1,2*], Martin R. Dixon[1], Johan Kroon[1], Timothy J. Hawkins[1], and Patrick J. Hussey[1ǂ].

[1]Department of Biosciences, Durham University, South Road, Durham, DH1 3LE, UK.
[2]College of Life and Environmental Sciences, University of Exeter, Stocker Road, Exeter, EX4 4QD, UK.
* these authors contributed equally to this manuscript
ǂ corresponding author.

Author for correspondence:
Patrick J Hussey
Tel: +44 (0) 191 33 41335
Email: p.j.hussey@durham.ac.uk

Figures and Tables:

Figures: 6 figures (all to be reproduced in colour).
Supporting Information: 6 figures and 3 tables.

Word Count: 4177

Summary

- During fertilisation, Pollen Receptor-Like Kinases (PRKs) control pollen tube growth through the pistil in response to extracellular signals, and regulate the actin cytoskeleton at the tube apex to drive tip growth.

- We investigated a novel link between membrane-integral PRKs and the actin cytoskeleton, mediated through interactions between PRKs and NET2A; a pollen-specific member of the NETWORKED superfamily of actin-binding proteins.

- We characterise NET2A as a novel actin-associated protein that localises to punctae at the plasma membrane of the pollen tube shank, which are stably associated with cortical longitudinal actin cables. NET2A was demonstrated to interact specifically with PRK4 and PRK5 in *Nicotiana benthamiana* transient expression assays, and associated at discreet foci at the shank membrane of Arabidopsis pollen tubes. Our data indicates NET2A is recruited to the plasma membrane by PRK4 and PRK5, and that PRK kinase activity is important in facilitating its interaction with NET2A.

- We conclude that NET2A-PRK interactions mediate discreet sites of stable interactions between the cortical longitudinal actin cables and plasma membrane in the shank region of growing

pollen tubes, which we have termed Actin-Membrane Contact Sites (AMCSs). Interactions between PRKs and NET2A implicate a role for NET2A in signal transduction to the actin cytoskeleton during fertilisation.

Keywords

Actin, Cytoskeleton, Fertilisation, Membrane, NET2A, Pollen, PRK, Signalling.

Introduction

Pollen tube growth is a critical step of fertilisation during the angiosperm reproductive cycle, and facilitates the delivery of non-motile sperm cells to the female gamete. It is known that the growing tube is guided through the pistil to the ovules by a large number of secreted signalling molecules, to ensure the targeting of pollen tube growth to the egg (Qu *et al*., 2015a); however our knowledge of the mechanisms controlling pollen tube growth and guidance during fertilisation remain limited.

The actin cytoskeleton is crucial for pollen tube growth (Gibbon *et al*., 1999; Vidali *et al*., 2001); driving cytoplasmic streaming (Vidali *et al*., 2001) and targeting of Golgi-derived secretory vesicles to the growing tip (Vidali & Helper, 2001; Lee *et al*., 2008; Rounds *et al*., 2014), whilst actin-dependent exocytosis and endocytosis also occurs in the pollen tube shank region (Moscatelli *et al*., 2012). To achieve polarised cell growth, the actin cytoskeleton has a highly organised and distinctive structure in growing pollen tubes. In the shank region of the tube, (corresponding to the non-growing region, >4 µm from the tip; Qu *et al*., 2017), filamentous actin (F-actin) is arranged into thick longitudinal actin cables, co-ordinating rapid, long range transport of organelles (Chen *et al*., 2009; Qu *et al*., 2015b). At the apical zone, (corresponding to the growing region, <4 µm from the tip; Qu *et al*., 2017), a distinct and highly dynamic population of longitudinally-aligned actin filaments coordinate tip growth and turning: cortical filaments drive and define the direction of tip growth through targeted apical exocytosis, and cytoplasmic filaments prevent retrograde movement of vesicles (Kost *et al*., 1999, Lovy-Wheeler *et al*., 2005; Lee *et al*., 2008; Chen *et al*., 2009; Qu *et al*., 2017). This

highly distinctive actin structure is regulated by a large number of actin-binding proteins, which regulate actin dynamics and organisation (Hussey *et al*., 2006; Staiger *et al*., 2010; and Qu *et al*., 2015b).

During fertilisation, the pollen tube actin cytoskeleton must be regulated in response to extracellular signals to drive pollen tube growth and navigation in the pistil. The actin cytoskeleton of pollen tubes is regulated by Pollen Receptor-Like Kinases (PRKs); a family of transmembrane leucine-rich repeat (LRR) receptor-like kinases (RLKs), with important roles in fertilisation (Lee *et al*., 1996; Takeuchi & Higashiyama, 2016). PRKs are known to influence pollen tube growth (Chang *et al*., 2013), downstream of binding external signalling ligands (Tang *et al*., 2002; Tang *et al*., 2004; Wengier *et al*., 2010; Huang *et al*., 2014) and mediate pollen tube navigation towards pistil-secreted guidance cues (Takeuchi & Higashiyama, 2016), demonstrating their importance as upstream surface regulators of pollen tube growth. PRKs have been implicated as regulators of the actin cytoskeleton through their involvement with Rop (Rho of plants) GTPases; molecular switches that control tip extension through the ROP-interactive CRIB-containing protein 3 (RIC3)/RIC4 pathway, which co-ordinates actin dynamics at the pollen tube apex (Fu *et al*., 2001; Gu *et al*., 2005; Zhang & McCormick, 2007; Lee *et al*., 2008; Chang *et al*., 2013, Takeuchi & Higashiyama, 2016). Therefore, PRKs are thought to control pollen tube growth downstream of external guidance signals through regulation of actin at the tube apex. However, the mechanisms of signal transduction to the pollen tube actin cytoskeleton by PRKs are only recently becoming understood, and it is likely that novel regulatory links

between PRKs and actin have yet to be discovered. Moreover, these cited studies have focused on the coupling of actin dynamics to the growing plasma membrane and trafficking at the tip, but have not revealed how villin and fimbrin-bundled actin of the shank interfaces with the older membrane and maturing cell wall.

Here, we report the identification of a novel link between PRK membrane receptors and the actin cytoskeleton, mediated by the actin-binding NET2 proteins. The NET2 proteins are a pollen-expressed subclade of the NETWORKED superfamily of actin-binding proteins, which bind actin filaments at various membrane compartments through their conserved N-terminal NAB (NET actin-binding) domains (Deeks *et al*., 2012; Wang *et al*., 2014). Members of the NET2 subfamily localise to discreet foci at the plasma membrane of the pollen tube shank, at which they bind both integral membrane protein kinases, PRK4 and PRK5, and cortical longitudinal actin cables. Furthermore, these results indicate that the NET2 proteins are regulated by PRKs to mediate stable points of contact between the plasma membrane and actin filaments in the pollen tube shank, which we have termed 'actin-membrane contact sites (AMCS)'.

Our data identify a role for NET2A in forming links with specific PRKs, raising the possibility that this connection at the AMCS acts as a platform for the transduction of extracellular signals to the actin cytoskeleton during fertilisation.

Materials and Methods

Plant material and transformations

Arabidopsis thaliana (L.) Heynh. (col-0) ecotype was used for the generation of stable Arabidopsis transformants using the floral dipping method according to Zhang *et al*., (2006). Seeds were grown on ½ Murashige & Skoog (MS) agar or compost in a growth chamber with a 16-hour day and 8-hour night cycle, with 22 ºC day temperature and 18 ºC night temperature.

Transient transformation of *Nicotiana benthamiana* was performed using leaf infiltration as described Sparkes *et al*., (2006). Plants were grown in a growth chamber with a 16-hour day and 8-hour night cycle, with 25 ºC day temperature and 18 ºC night temperature.

Molecular cloning and vectors

cDNAs of full-length NET2A, NET2B, PRK1, PRK2, PRK3, PRK4, PRK5, PRK6, were amplified from total floral cDNA using polymerase chain reaction (PCR), with the primers listed in table S1. Coding sequences of respective subdomains and truncations of these proteins were also amplified from these cDNA templates using the primers list in table S1. The cDNAs were transiently expressed in *N. benthamiana* leaf epidermal cells as fluorescent fusion proteins by cloning them into various binary gateway vectors using the gateway cloning system (Invitrogen). pB7FGW2 for C-terminal green fluorescent protein (GFP), pH7RGW2 for C-terminal red fluorescent protein (RFP) and pMDC83-mCherry for (C-terminal mCherry) were used.

For stable expression of PRK4 and PRK5 as fluorophore fusions under the *pLAT52* promoter, pB7FGW52 (C-terminal GFP) and pH7RGW52 (C-terminal RFP) were used.

The expression vectors pMDC83-mCherry, pB7FGW52 and pH7RGW52 were generated using restriction subcloning. To generate pMDC83-mCherry, the mCherry coding sequence was PCR amplified with added 5'*AscI* and 3'*BstBI* restriction sites using the primers listed in table S1. *AscI*/*BstBI* double restriction digest of pMDC83 was performed to excise the GFP coding sequence, and ligation of 5'-*AscI*-mCherry-*BstBI*-3' into the pMDC83 *AscI*/*BstBI* site was performed using T7 DNA ligase (NEB). To generate pB7FGW52 and pH7RGW52, the *pLAT52* promoter sequence (Twell *et al*., 1990) was PCR amplified with added 5'*SacI* and 3'*SpeI* sites using the primers described in table S1. Excision of the *CaMV 35s*: promoter sequence was performed using *SacI*/*SpeI* double restriction digest, and the 5'-*SacI*-*pLAT52*-*SpeI*-3' DNA fragment was ligated into the excision site using T7 DNA ligase (NEB).

To generate the PRK5^{K403R} kinase-dead PRK5 mutant construct (in which Lysine-403 of PRK5 was mutagenised to Arginine), site-directed mutagenesis was performed on the full-length, wild-type PRK5 coding sequence using the QuickChange II Site Directed Mutagenesis Kit (Agilent). The codon for Lysine-403 was altered to Arginine using the primers listed in table S1.

Live cell imaging and FRET-FLIM

Transiently transformed *N. benthamiana* leaves were imaged 4 days after infiltration using laser scanning confocal microscopy (LSCM; Leica TCS SP5). Images were acquired in multi-track mode with line switching when imaging co-localisation of multiple fluorophores. For drug treatments, leaf sections were incubated in 50 µM Latrunculin B (30 minutes) or 50 µM amiprophos methyl (APM; 2 hours) to disrupt actin or microtubules respectively.

Förster resonance energy transfer-fluorescence lifetime imaging microscopy (FRET-FLIM) was performed using the Leica TCS SP5 SMD LSCM combined with fluorescence lifetime system (PicoQuant). Data analysis and acquisition was performed with SymPhoTime software (PicoQuant). The lifetime of the donor construct expressed alone was measured as a negative control, and compared to the lifetime of the donor when co-expressed with the acceptor construct. The GFP fluorescence lifetimes of GFP-RFP and GFP-mCherry fusion proteins were measured as a positive control. All measurements were taken from whole-field images of cells expressing fluorophore fusion proteins at similar levels.

Yeast-2-hybrid (Y2H)

The intracellular domains of PRK1, PRK2, PRK3, PRK4, PRK5 and PRK6 were PCR amplified using the primers listed in table S1. The cDNAs were cloned into pGBKT7 (Clontech) using gateway cloning (Invitrogen), to facilitate their expression as bait protein constructs. The full-length NET2A cDNA was cloned into pGADT7 (Clontech) using

the gateway cloning system (Invitrogen) to facilitate its expression as prey protein constructs.

The pGBKT7 constructs were transformed into the MATα Saccharomyces cerevisiae strain Y187 (Clontech), and pGADT7 constructs were transformed into the MATa strain, AH109 (Clontech) using the manufacturer's instructions.

NET2A in pGADT7 was mated against each pGBKT7 construct on yeast peptone dextrose adenine (YPDA) media at 28 ºC for 24 hours, and diploids containing both constructs were selected on standard defined (SD) media lacking Leucine and Tryptophan. Interactions between bait and prey protein constructs was assessed by selecting diploid yeast on SD media also lacking Histidine, and supplemented with 2.5 mM 3-Amino-1,2,4-triazole (3AT). As negative controls, pGADT7 constructs were mated against empty pGBKT7, and pGBKT7 constructs were mated against empty pGADT7.

In vitro pollen germination and observation

Arabidopsis pollen was germinated *in vitro* on solid germination media as described by Li *et al*., (1999). Germination media consisted of 18 (w/v) % sucrose, 0.01 % (w/v) H_3BO_4, 1 mM $Ca(NO_3)_2$, 1 mM $MgSO_4$, 1 mM $CaCl_2$, and 0.5 % (w/v) Agarose Type VII-A (Sigma), pH 7. Mature Arabidopsis pollen was dusted onto the solid germination media. 3 - 4 excised Arabidopsis pistils were placed on surface of the media and samples were incubated in a dark humid environment at 22 ºC for > 4 hours. Subsequently, germinated pollen was analysed using LSCM as described above.

Results

All members of the Arabidopsis NET2 subfamily co-localise with actin filaments *in vivo*

The NET proteins represent a novel superfamily of actin-binding proteins which we have shown to associate with actin through their conserved N-terminal NAB domains (Deeks *et al*., 2012; Wang *et al*., 2014). Accordingly, the NAB domain is highly conserved in each member of the NET2 subclade (Fig. 1a; Hawkins *et al*., 2014), indicating that they are also likely to bind actin directly. Here, we show each member of the NET2 subfamily has the ability to associate with F-actin *in vivo*. GFP fusions of the NET2A NAB domain were observed to localise to actin filament networks when transiently expressed in *N. benthamiana* (a simple experimental system for rapid expression and analysis of fluorescently-tagged proteins). NET2A-GFP co-localised with the F-actin marker, RFP-lifeact (Fig. 1b), and this localisation was disrupted by treatment with actin-targeting drugs (Fig. 1c). Likewise, GFP fusions of the NET2B, NET2C and NET2D NAB domains also localised to actin filaments *in vivo* (Fig. 1d), effectively demonstrating each NET2 subfamily member can localise to F-actin through their N-terminal NAB domains. It was observed that full-length NET2A-GFP and NET2B-GFP also localised to actin filaments when transiently expressed in *N. benthamiana leaves*: 90.7 ± 2.3 % NET2A-GFP punctae co-localised with actin filaments, decorating them in the 'beads-on-a-string pattern', as is characteristic of NET superfamily proteins (Fig. 1e, Fig. S1; Deeks *et al*., 2012). Taken together, our data indicates that each member of the NET2 subclade is

able to localise to F-actin *in vivo*, through their N-terminal NAB domains.

NET2A co-localises with F-actin at the pollen tube plasma membrane

Having determined the ability of the NET2 proteins to localise to the actin cytoskeleton in transient leaf transformation, it was then investigated as to whether they may also co-localise with actin filaments *in situ*. Therefore, we analysed NET2A-GFP in Arabidopsis pollen tubes (the NET2 proteins' endogenous environment). Previously, we have demonstrated that native promoter-driven NET2A-GFP localises to discreet punctae specifically at the shank region of the pollen tube plasma membrane (Deeks *et al*., 2012; Fig. 2a & 2b). Here, we demonstrate that these NET2A foci co-localise with cortical F-actin cables at the shank membrane of the pollen tube. The NET2A-GFP punctae aligned along actin cables stained with the F-actin probe, rhodamine-phalloidin (Fig. 2c), and co-localised with F-actin filaments in live pollen tubes co-expressing native promoter-driven NET2A-GFP and the genetically encoded actin-marker construct, FABD2-RFP, stably expressed in pollen under the pollen-specific promoter, *pLAT52* (Fig. 2d; Twell *et al*., 1990). The NET2A punctae decorated actin filaments in the characteristic 'beads-on-a-string' pattern typical of NET superfamily proteins, and 80.2 ± 6.1 % of NET2A-GFP punctae were observed to co-localise with FABD2-RFP-labelled actin filaments. Using rapid time-lapse imaging, we observed the localisation of NET2A-GFP punctae at the plasma membrane to be highly stable and persist at the

membrane throughout pollen tube growth (video S1). The punctae were not highly motile, but appeared to undergo abrupt, co-ordinated, short-range, anterograde and retrograde movements along linear vectors (Fig. S2). This indicates that NET2A localises to stable punctae at the pollen tube cortex. Taken together, these data show that NET2A forms stable associations with cortical actin filaments at the pollen tube membrane.

NET2A interacts specifically with PRK isoforms 4 and 5

Our data showed that F-actin localisation is conferred by the NAB domains of NET2 proteins, however it remained unknown how actin-localised foci of full-length NET2A are recruited to the plasma membrane as NET proteins do not contain transmembrane domains or identifiable modification sites associated with known peripheral membrane proteins. A potential orthologue of the NET2 proteins in Petunia, *Petunia inflata* Kinase Interacting Protein 1 (PiKIP1), has been identified as an interactor of PRK proteins in a Y2H screen using *Petunia inflata* Pollen Receptor-Like Kinase 1 (PiPRK1) as bait (Skirpan *et al*., 2001). Importantly, PiKIP1 was not characterised as a NET-family actin-binding protein. PRKs are integral membrane proteins, suggesting the hypothesis that PRKs contribute to NET2 membrane recruitment. We used combinatorial Y2H to test the potential for interactions between Arabidopsis NET2 and PRK family members. Full-length NET2A was observed to interact with the cytosolic domains of PRK4 and PRK5 (Fig. 3a) but did not interact with PRK1, PRK2, PRK3 or PRK6 (Fig. S3). Interestingly, PRK4 and PRK5 belong to a distinct

evolutionary subclade of PRKs (Chang *et al*., 2013; Takeuchi & Higashiyama., 2016), suggesting that the NET2 family show sequence-based isoform specificity in this assay.

We then sought to validate NET2 kinase interactions *in planta* using FRET-FLIM, NET2A-mCherry interacted specifically with PRK4-GFP and PRK5-GFP in FRET-FLIM assays when transiently expressed in *N. benthamiana* leaf tissue. When co-expressed with NET2A-mCherry, the average fluorescence lifetime of PRK4-GFP was reduced by 0.23 ns to 2.22 ± 0.06 ns compared to the control (2.45 ± 0.02 ns). Similarly, the fluorescence lifetime of PRK5-GFP was reduced by 0.36 ns to 2.15 ± 0.02 ns compared to the control (2.51 ± 0.02 ns; Fig. 3b), sufficient to demonstrate an interaction (Danquah *et al*., 2011; Wang *et al*., 2014). Consistent with the Y2H data, NET2A-mCherry did not interact with PRK1-GFP, PRK2-GFP, PRK3-GFP or PRK6-GFP (table S2). Interestingly, we also observed NET2B to interact specifically with PRK4 and PRK5 using FRET-FLIM (table S3). Our data therefore shows that multiple NET2 subfamily members interact specifically with the PRK4/PRK5 subclade of Arabidopsis PRKs *in planta*.

NET2s are recruited to the plasma membrane by PRK4 and PRK5.

Transient co-expression of NET2A-GFP with either PRK4-RFP or PRK5-RFP in *N. benthamiana* leaves resulted in striking changes in NET2A-GFP subcellular localisation. Whereas NET2A-GFP localised to punctae and filaments when expressed alone, it was found distributed exclusively at the plasma membrane when co-

expressed with PRK5-GFP (Fig. 4a, Fig. S4); where the two proteins could be observed to co-localise (Fig. 4b). When co-expressed with PRK4-RFP, NET2A-GFP localised to the plasma membrane and peripheral cytosol (Fig. 4a). As a negative control, the subcellular localisation of NET2A-GFP was analysed when co-expressed with PRK6-RFP (no interactions between NET2A and PRK6 were detected in Y2H or FRET-FLIM assays; Fig. S3, Table S2). Importantly, NET2A-GFP was observed to remain localised to filaments and punctae and did not localise to the plasma membrane (Fig. S5). Furthermore, it was also observed that like NET2A-GFP, NET2B-GFP could also be recruited to the plasma membrane by PRK4-RFP and PRK5-RFP specifically (Fig. S6).

To further investigate how PRK4 and PRK5 interact with NET2 proteins, we analysed the specific subdomains of the PRKs that mediate the interaction with NET2A. Truncated PRK mutants lacking intracellular C-terminal kinase domains (PRKΔK) were generated (Fig. 4c). RFP fusions of PRK4ΔK (PRK4$^{1\text{-}374}$) and PRK5ΔK (PRK5$^{1\text{-}376}$) were unable to recruit NET2A-GFP to the plasma membrane, which instead localised to punctae and filaments in a similar manner to NET2A-GFP expressed alone (Fig. 4d). FRET-FLIM indicated no interaction between NET2A-GFP and PRK5ΔK-RFP (Fig. 4e), suggesting that PRKs bind and recruit NET2 proteins to the membrane through their cytoplasmic kinase domain.

We then investigated specific residues of PRK5 important in mediating the interaction with NET2A. *in vitro* experiments have indicated that phosphorylation of petunia PiKIP1 by PiPRK1 contributes to the interaction between the two proteins, and kinase-dead mutant

variants of PiPRK1 are diminished in their ability to bind PiKIP1. Lysine-403 of PRK5, (homologous to PiPRK1 Lysine-462; predicted to be important for kinase Mg^{2+}/ATP binding; Skirpan *et al*., 2001) was replaced by Arginine to generate $PRK5^{K403R}$. It was observed that the $PRK5^{K403R}$-RFP construct recruited NET2A-GFP to the plasma membrane when co-expressed in *N. benthamiana* leaf epidermal cells, similar to WT PRK5-RFP. However, $PRK5^{K403R}$-RFP showed reduced resonance with NET2A-GFP in the FRET-FLIM system (Fig. 4g). When co-expressed, the full length PRK5-RFP construct induced a decrease in average NET2A-GFP fluorescence lifetime of 0.38 ns to 2.10 ± 0.07 ns, compared to the control (2.48 ± 0.08 ns). In comparison, $PRK5^{K403R}$-RFP induced only a small decrease in average NET2A-GFP fluorescence lifetime of 0.14 ns to 2.34 ± 0.05 ns, suggestive of a relatively weak interaction. This indicates that Lysine-403 of PRK5 is important in facilitating the interaction between PRK4/PRK5 and NET2s *in vivo*. We speculate that PRK5 Lysine-403 is functionally equivalent to PiPRK1 Lysine-462 and may be important for PRK5 kinase activity, which is likely to mediate an interaction with NET2A.

Taken together, the data suggests that specific members of the PRK family, namely PRK4 and PRK5, are able to bind, and recruit NET2 proteins to the plasma membrane *in vivo* through their intracellular kinase domains.

NET2A associates with PRK4 and PRK5 at discreet foci at the plasma membrane of the pollen tube shank

We have shown that NET2 proteins associate with actin filaments and can be recruited to the plasma membrane through interactions with specific PRKs in leaf transient expression assays. However, NET2A forms punctae at the plasma membrane of the pollen tube shank. We therefore asked whether populations of PRK4 and PRK5 coincide with these punctae in growing pollen tubes. We observed PRK4-GFP and PRK5-GFP localised to discreet foci at the pollen tube plasma membrane (Fig. 5), with a similar pattern: the average puncta size for both PRK4-GFP and PRK5-GFP was observed to be highly similar (average PRK4-GFP puncta size = 0.47 ± 0.11 µm, average PRK5-GFP puncta size = 0.46 ± 0.10 µm), as was the density of PRK4-GFP and PRK5-GFP punctae at the shank plasma membrane (PRK4-GFP punctae density = 0.65/µm^2, PRK5-GFP punctae density = 0.62/µm^2). The PRK4-GFP and PRK5-GFP punctae were, alike, distributed along the membrane of the pollen tube shank region but were reduced in intensity at the growing tip (both were visible only at distances greater than ≈ 15 µm distal to the apex), in a manner highly similar to those of NET2A-GFP (Fig. 2). Therefore, it was investigated as to whether NET2A may associate with PRK4 and PRK5 at these membrane foci. The results show that NET2A-GFP and PRK4-RFP co-localise to the same punctae at discreet foci at the pollen tube membrane in stable transgenic Arabidopsis lines expressing native promoter-driven NET2A-GFP and PRK4-RFP (Fig. 6). In pollen tubes co-expressing NET2A-GFP and PRK4-RFP under *pLAT52*, we observed 83.0 ± 7.3 % of NET2A-GFP punctae co-

localised with PRK4-RFP punctae (n = 265 punctae in 6 cells). Taken together with the yeast 2-hybrid and FRET-FLIM experiments, these data show that NET2A co-localises with PRK4/PRK5 punctae at the pollen tube membrane, representing discreet sites of interaction between NET2A and PRK proteins at the plasma membrane of the pollen tube shank.

Discussion

Our data demonstrates a novel mechanism of interaction between the actin cytoskeleton and the pollen tube plasma membrane, in which NET2 proteins bind actin filaments to the plasma membrane through association with the membrane-integral pollen receptor-like kinases, PRK4 and PRK5. This discovery suggests that the NET2 proteins have an important role in angiosperm fertilisation and in the regulation of the actin cytoskeleton in response to extracellular signals. In this context, whilst it is known that PRKs control actin dynamics at the pollen tube apex (Zhang & McCormick, 2007; Lee *et al*., 2008; Chang *et al*., 2013; Takeuchi & Higashiyama, 2016), nothing is known about how the cortical longitudinal actin cables of the pollen tube shank may be regulated at the plasma membrane in response to external signals. This unique subpopulation of actin filaments has specialised functions in mediating rapid, long-range anterograde, cytoplasmic streaming (Chen *et al*., 2009; Qu *et al*., 2015b), and their specific association with NET2A indicates importance of their regulation in response to external signals, and an interesting role for NET2 proteins in their organisation downstream of PRK signalling.

The NET2 proteins represent a subclade of the NETWORKED superfamily of actin-binding proteins, which associate with actin filaments at various organelle membranes through their N-terminal NAB domains (Deeks *et al*., 2012). Accordingly, we have demonstrated that the NET2 proteins are, likewise, proteins that co-localise with F-actin *in vivo* through their conserved NAB domains, as GFP fusions of each NET2 NAB domain and full-length NET2 proteins were observed to localise to actin filaments *in vivo*. Consistent with other NET superfamily proteins, we show members of the NET2 subfamily to bind actin at cellular membranes: NET2A was observed to localise to discreet foci at the pollen tube plasma membrane, which aligned along actin-filaments. Taken together, we conclude that NET2A associates with cortical actin at the plasma membrane of the pollen tube shank.

Our data suggests that NET2 proteins bind cortical F-actin at the membrane through association with PRK4 and PRK5 at discreet foci, which we have termed ‘actin-membrane contact sites (AMCSs)’. During this investigation, we determined that NET2s interact specifically with the PRK4/PRK5 subclade of PRKs (but not PRK1, PRK2, PRK3, or PRK6), in Y2H and FRET-FLIM assays. In growing pollen tubes PRK4 and PRK5 localise to punctae in a similar distribution, specifically in the mature regions of the growing pollen tube, at which co-localisation with NET2A was observed. Therefore, NET2A interacts with PRK4 and PRK5 at the pollen tube plasma membrane at discreet foci.

In transient expression assays, it was noted that PRK4 and PRK5 recruit NET2s to the plasma membrane: we therefore hypothesise that NET2s bind actin filaments at

602 the cell cortex through their associations with PRK4 and
603 PRK5 at the pollen tube plasma membrane to form
604 AMCSs. AMCSs appear to be persistent structures, and
605 NET2A punctae were observed to localise permanently to
606 the shank membrane, indicating their associations with
607 PRKs to be highly stable. AMCSs formed by NET2-PRK
608 interactions may therefore serve as stable membrane
609 anchors for actin filaments, with roles in the organisation
610 of cortical longitudinal actin cables in the pollen tube
611 shank.

612 Through their associations with PRKs, the NET2
613 subfamily may be implicated as having roles in
614 extracellular signal transduction to the cytoskeleton
615 during fertilisation. PRKs are believed to be important in
616 fertilisation and transduce a number of extracellular
617 signals to direct pollen tube growth to the female gamete.
618 Notably, PRK4 and PRK5 recognise and transduce the
619 extracellular signalling peptide, GRIM REAPER (GRI): an
620 orthologue of *Lycopersicum esculentum* STIGMA-
621 SPECIFIC 1 (LeSTIG1; Wrzaczek *et al*., 2009), which
622 promotes pollen tube growth downstream of binding
623 tomato LePRK2 (Tang *et al*., 2004; Huang *et al*., 2014).
624 During fertilisation, PRK4 and PRK5 may promote pollen
625 tube growth in the stigma in response to binding
626 members of the STIG1 family. Considering this, it is
627 tempting to speculate that NET2A may regulate the actin
628 cytoskeleton downstream of PRK4 and PRK5 to facilitate
629 STIG1-stimulated pollen tube growth. Our data indicates
630 that the kinase activity of PRK5 is important in promoting
631 its interaction with NET2A. Consistent with this,
632 phosphorylation of PiKIP1 by PiPRK1 has been shown to
633 be important for interactions to occur between the two
634 proteins (Skirpan *et al*., 2001). It is therefore probable

that NET2A is phosphorylated by PRK5 and may serve as a downstream signalling effector. In Arabidopsis, other PRKs such as PRK2, PRK3 and PRK6 are believed to regulate cytoskeletal dynamics downstream of ligand binding to control pollen tube growth through the Rop signalling pathway, specifically at the pollen tube apex (Chang *et al*., 2013; Zhao *et al*., 2013; Takeuchi & Higashiyama, 2016). Importantly, here we have identified an additional mechanism by which unique PRKs may regulate the actin cytoskeleton through NET2A; distinct from apical Rop signalling and spatially localised to the shank region of the tube. We propose that PRK4 & PRK5 may regulate the cortical longitudinal actin cables of the pollen tube shank in response to extracellular signals, during fertilisation.

Acknowledgements

The work was supported by a BBSRC grant (BB/G006334/1) to P.J.H. The DNA template for the *pLAT52* promoter sequence was kindly provided by Professor David Twell, University of Leicester.

Author Contributions

PJH conceived the project, which was supervised by MJD and PJH. Most of the experiments were performed by PD, with exception of the cloning and expression of the NET2 NAB domains, generation of *pLAT52*:FABD2-RFP stable transgenic lines and rhodamine-phalloidin staining of *pNET2A*:NET2A-GFP pollen tubes (performed by MRD). Generation of *pNET2A*:NET2A-GFP stable transgenic lines was performed by MJD, and generation

of the PRK5^{K403R} construct was performed by JK. PD prepared the figures and wrote the manuscript with MJD, TJH and PJH.

References

Chang F, Gu Y, Ma H, Yang Z. 2013. AtPRK2 promotes ROP1 activation via RopGEFs in the control of polarized pollen tube growth. *Mol Plant* **6**: 1187 – 1201.

Chen N, Qu X, Wu Y, and Huang S. 2009. Regulation of actin dynamics in pollen tubes: control of actin polymer level. *J. Integr. Plant Biol* **51**: 740 – 750.

Danquah JO, Botchway S, Jeshtadi A, King L. 2012. Direct interaction of Baculovirus Capsid proteins VP39 and EXON0 with Kinesin-1 in insect cells determined by fluorescence resonance energy transfer-fluorescence lifetime imaging microscopy. *J Virol*. **86**: 844 – 853.

Deeks, M, Calcutt JR, Ingle ES, Hawkins TJ, Chapman S, Richardson AC, Mentlak DA, Dixon MR, Cartwright F, Smertenko AP, *et al*. 2012. A superfamily of actin-binding proteins at the actin-membrane nexus of higher plants. *Current Biology* **22**: 1595 – 600.

Fu Y, Wu G, Yang Z. 2001. ROP GTPase–dependent dynamics of tip-localized F-actin controls tip growth in pollen tubes. *J Cell Biol* **152:** 1019 – 1032.

Gibbon BC, Kovar DR, Staiger CJ. 1999. Latrunculin B has different effects on pollen germination and tube growth. *Plant Cell* **11:** 2349 – 2363.

Gu Y, Fu Y, Dowd P, Li S, Vernoud V, Gilroy S, Yang Z. 2005. A Rho family GTPase controls actin dynamics and tip growth via two counteracting downstream pathways in pollen tubes. *J Cell Biol* **169**: 127 – 138.

Hawkins TJ, Deeks MJ, Wang P, Hussey PJ. 2014. The evolution of the actin binding NET superfamily. *Front Plant Sci*. doi: 10.3389/fpls.2014.00254.

Huang WJ, Liu HJ, McCormick S, Tang WH. 2014. Tomato pistil factor STIG1 promotes *in vivo* pollen tube growth by binding to phosphatidylinositol 3-phosphate and the extracellular domain of the pollen receptor kinase LePRK2. *Plant Cell* **26**: 2505 – 2523.

Hussey PJ, Ketelaar T, Deeks M.J. 2006. Control of the actin cytoskeleton in plant cell growth. *Annual Review of Plant Biology* **57**: 109 – 125.

Kost B, Mathur J, Chua NH. 1999. Cytoskeleton in plant development. *Curr Op Plant Biol* **2**: 462 - 470.

Lee HS, Karunanandaa B, McCubbin A, Gilroy A, Kao TH. 1996. PRK1, a receptor-like kinase of *Petunia inflata*, is essential for postmeiotic development of pollen. *Plant Journal* **9**: 613 – 624.

Lee, YJ, Szumlanski A, Nielsen E, and Yang ZB. 2008. Rho-GTPase dependent filamentous actin dynamics coordinate vesicle targeting and exocytosis during tip growth. *J. Cell Biol* **181:** 1155 – 1168.

Li H, Lin Y, Heath RM, Zhu MX, Yang Z. 1999. Control of pollen tube tip growth by a Rop GTPase-dependent pathway that leads to tip-localized calcium influx. *Plant Cell* **11**: 1731 – 1742.

Lovy-Wheeler A, Wilsen KL, Baskin TI, Hepler PK. 2005. Enhanced fixation reveals the apical cortical fringe of actin filaments as a consistent feature of the pollen tube. *Planta* **221**: 95 – 104.

Moscatelli A, Idiili A, Rodighiero S, Caccianiga M. 2012. Inhibition of actin polymerisation by low concentration Latrunculin B affects endocytosis and alters exocytosis in shank and tip of tobacco pollen tube. *Plant Biology* **14**: 770 – 782.

Qu LJ, Li L.Lan Z, Dresselhaus T. 2015a. Peptide signalling during the pollen tube journey and double fertilization. *J Exp Bot*. **66**: 5139 – 5150.

Qu X, Jiang Y, Chang M, Liu X, Zhang R, Huang S. 2015b. Organisation and regulation of the actin cytoskeleton in the pollen tube. *Front Plant Sci.* doi: 10.3389/fpls.2014.00786.

Qu X, Zhang R, Zhang M, Diao M, Xue Y, Huang S. 2017. Organizational innovation of apical actin filaments drives rapid pollen tube growth and turning. *Mol Plant*. **10:** 930 - 947

Rounds CM, Hepler, PK, Winship LJ. 2014. The apical actin fringe contributes to localized cell wall deposition and polarized growth in the lily pollen tube. *Plant Physiol* **166**: 139 – 151.

Skirpan AL, McCubbin AG, Ishimizu T, Wang X, Hu Y, Dowd PE, Ma H, Kao TH. 2001. Isolation and characterization of kinase interacting protein 1, a pollen protein that interacts with the kinase domain of PRK1, a receptor-like kinase of Petunia. *Plant Physiology* **126:** 1480 - 1492.

Sparkes IA, Runions J, Kearns A, Hawes C. 2006. Rapid, transient expression of fluorescent fusion proteins in tobacco plants and generation of stably transformed plants. *Nat Prot* **1**: 2019 – 2025.

Staiger CJ, Poulter NS, Henty JL, Franklin-Tong VE, Blanchoin L. 2010. Regulation of actin dynamics by actin-binding proteins in pollen. *J Exp Bot* **61**, 1969 – 1986.

Takeuchi H, Higashiyama T. 2016. Tip-localized receptors control pollen tube growth and LURE sensing in *Arabidopsis*. *Nature* **531:** 245 – 248.

Tang W, Kelley D, Ezcurra I, Cotter R, McCormick S. 2004. LeSTIG1, an extracellular binding partner for the pollen receptor kinases LePRK1 and LePRK2, promotes pollen tube growth *in vitro*. *Plant J* **39**: 343 – 353.

Tang W, Ezcurra I, Muschietti J, McCormick S. 2002. A cysteine-rich extracellular protein, LAT52, interacts with the extracellular domain of the pollen receptor kinase LePRK2. *Plant Cell* **14**: 2277 – 2287.

Twell D, Yamaguchi J, McCormick S. 1990. Pollen-specific gene expression in transgenic plants: coordinate regulation of two different tomato gene promoters during microsporogenesis. *Development* **109**: 705 – 713.

Wengier DL, Mazzella, MA, Salem TM, McCormick S, Muschietti JP. 2010. STIL, a peculiar molecule from styles, specifically dephosphorylates the pollen receptor kinase LePRK2 and stimulates pollen tube growth *in vitro. BMC Plant Biol* **10**: 33, DOI: 10.1186/1471-2229-10-33.

Wrzaczek M, Broschéa M, Kollista H, Kangasjärvi J. 2009. *Arabidopsis* GRI is involved in the regulation of cell death induced by extracellular ROS. *PNAS* **106**: 5412 – 5417.

Wrzaczek M, Vainonen JP, Stael S, Tsiatsiani L, Help-Rinta-Rahko H, Gauthier A, Kaufholdt D, Bollhöner B, Lamminmäki A, Staes A, *et al.* 2015. GRIM REAPER peptide binds to receptor kinase PRK5 to trigger cell death in *Arabidopsis*. *EMBO J* **34**: 55 – 66.

Vidali L, Hepler PK. 2001. Actin and pollen tube growth. *Protoplasma* **215**: 64 - 76.

Vidali L, Mckenna ST, Hepler PK. 2001. Actin polymerization is essential for pollen tube growth. *Mol Biol Cell* **12**: 2534 – 2545.

Wang P, Hawkins TJ, Richardson C, Cummins I, Deeks MJ, Sparkes I, Hawes C, Hussey PJ. 2014. The plant cytoskeleton, NET3C, and VAP27 mediate the link between the plasma membrane and endoplasmic reticulum. *Curr Biol* **24**: 1397 -1405.

Zhao XY, Wang Q, Li S, Ge FR, Zhou LZ, McCormick S, Zhang Y. 2013. The juxtamembrane and carboxy-terminal domains of *Arabidopsis* PRK2 are critical for ROP-induced growth in pollen tubes. *J Exp Bot* **64**: 5599 – 5610.

Zhang Y, McCormick S. 2007. A distinct mechanism regulating a pollen-specific guanine nucleotide exchange factor for the small GTPase Rop in *Arabidopsis thaliana*. *PNAS* **104:** 18830 – 18835.

Zhang X, Henriques R, Lin SS, Niu QW, Chua NH. 2006. *Agrobacterium*-mediated transformation of *Arabidopsis thaliana* using the floral dip method. *Nat Protoc* **1**: 641 – 646.

Figure Legends

Fig 1: NET2s belong to the NET superfamily of actin-binding proteins and localise to the actin cytoskeleton in *Nicotiana benthamiana* leaf epidermal cells through conserved N-terminal NET actin-binding (NAB) domains

(a) multiple alignment of the NET superfamily NAB domains. (b) NET2A-NAB-GFP co-localises with actin filaments *in vivo.* (c) disruption of the actin cytoskeleton using 40 µM Cytochalaisin D results in breakdown of NET2A-NAB-GFP filament network. (d) GFP fusions of NET2B, NET2C and NET2D NAB domains also localise to actin filaments *in vivo*. (e) full-length NET2A-GFP co-localises with actin-filaments *in vivo*. Scale bar = 10 µm.

Fig 2: NET2A localises to punctae at the pollen tube plasma membrane that co-localise with actin filaments

(a, b) subcellular localisation of natively expressed NET2A-GFP to the plasma membrane in growing

Arabidopsis pollen tubes (single z-plane images). (c) co-localisation of NET2A-GFP punctae with actin filaments in the Arabidopsis pollen tube shank, labelled with rhodamine-phalloidin. (d) co-localisation of NET2A-GFP punctae and the actin-marker, FABD2-RFP. 80.2 ± 6.1 % of NET2A-GFP punctae were observed to co-localise with FABD2-RFP-labelled actin filaments. Scale bar = 10 µm.

Fig 3: NET2A interacts with Arabidopsis PRK4 and PRK5

(a) NET2A interacts with PRK4 and PRK5 in yeast-2-hybrid assays. Yeast were grown on permissive media lacking Tryptophan and Leucine (-WL), or selective media lacking Tryptophan, Leucine and Histidine (–WLH). Yeast containing pGADT7-NET2A and pGBKT7-PRK4, or pGADT7-NET2A and pGBKT7-PRK5 were able to grow on selective media, indicating an interaction. Yeast containing pGADT7-NET2A and empty pGBKT7, empty pGADT7 and pGBKT7-PRK4, and empty pGADT7 and pGBKT7-PRK5 were used as negative controls and were unable to grow on selective media. (b) FRET-FLIM (Förster resonance energy transfer-fluorescence lifetime imaging microscopy) analysis of interactions between PRK4-GFP and NET2A-mCherry, and PRK5-GFP and NET2A-mCherry in *Nicotiana benthamiana* leaf epidermal cells. The average fluorescence lifetimes of the PRK4-GFP and PRK5-GFP donor constructs was reduced in the presence of the NET2A-mCherry acceptor construct, to comparable levels to the GFP-mCherry control. Images are pseudocoloured according to GFP fluorescence lifetime. Associated charts represent peak lifetime frequency of the acceptor construct in each image. A

leftward shift in peak lifetime frequency indicates a reduction in average GFP fluorescence lifetime. (c) diagrammatic representation of actin-membrane interactions mediated by NET2A and PRK4 & PRK5. Error bars on charts correspond to standard deviation.

Fig 4: PRK4 and PRK5 interact with NET2A through their cytosolic kinase domains and recruit NET2A to the plasma membrane in *Nicotiana benthamiana* leaf epidermal cells.

(a) co-expression of NET2A-GFP with PRK4-RFP or PRK5-RFP induces alterations in NET2A-GFP subcellular localisation in *N. benthamiana* transient assays. (b) NET2A-GFP co-localises with PRK5-RFP at the plasma membrane when both constructs are co-expressed together. (c) schematic diagrams of PRK4ΔK (PRK4 without the intracellular kinase domain) and PRK5ΔK (PRK5 without the intracellular kinase domain) truncation mutants. (d) NET2A-GFP does not localise to the plasma membrane when co-expressed with PRK4ΔK-RFP or PRK5ΔK-RFP. (e) NET2A-GFP does not interact with PRK5ΔK-RFP in FRET-FLIM (Förster resonance energy transfer-fluorescence lifetime imaging microscopy) interaction assays. (f) NET2A-GFP cannot be recruited to the membrane by PRKΔK mutants. (g) FRET-FLIM indicates the interaction between NET2A-GFP and PRK5-RFP is weakened in the $PRK5^{K403R}$ mutant (PRK5 with Lysine-403 replaced by Arginine). Scale bars: 10 μm. Error bars on charts correspond to standard deviation.

Fig 5: PRK4 and PRK5 localise to punctae at the plasma membrane of the pollen tube shank

(a) PRK4-GFP in Arabidopsis pollen tubes. (i) max projection of whole pollen tube. (ii) magnified image of PRK4-GFP punctae at the pollen tube shank (cortical section). (iii) magnified image of PRK4-GFP punctae at the pollen tube shank (cross-section). (b) PRK5-GFP in Arabidopsis pollen tubes. (i) cross section of whole pollen tube. (ii) magnified image of PRK5-GFP punctae at the pollen tube shank (cortical section). (iii) magnified image of PRK5-GFP punctae at the pollen tube shank (cross-section). Scale bars: (i) = 10 µm, (ii) and (iii) = 5 µm.

Figure 6: NET2A associates with PRKs at discreet foci at the shank plasma membrane of Arabidopsis pollen tubes

(a) NET2A-GFP punctae co-localise with PRK4-RFP punctae in Arabidopsis pollen tubes. Scale bar = 10 µm. (b) magnified image depicted by the inset in (a). Scale bar = 2 µm.

Supporting Information Legends

Fig. S1: NET2B-GFP subcellular localisation in *N. benthamiana* leaf epidermal cells.

Full-length NET2B-GFP localises to actin filaments in a beads-on-a-string pattern characteristic of NET proteins when expressed in *N. benthamiana* leaf epidermal cells. Scale bar: 10 µm.

Fig. S2: Kymograph of video S1 showing co-ordinated linear movement of NET2A-GFP patches.

The white line indicates the position of the kymograph which was taken over a width of 5 pixels.

(a) The kymograph shows movement initiating at approximately 270 s from time 0.

(b) (indicated by triangular arrowhead). Three neighbouring patches move in the retrograde direction. A 3 pixel kymograph along the centre line of the pollen tube shows that the NET2A patch distribution persists over long time scales.

(c) Patches form in a zone behind the growing tip. Nascent patches initiating during the duration of the time series are located in a zone marked by an asterisk. The white-bordered scale bar is 20 µm**.**

Fig. S3: Interactions between NET2A and Arabidopsis PRKs are restricted to PRK4 and PRK5 in Y2H assays, and NET2A is unable to interact with PRK1, PRK2, PRK3 or PRK6.

Yeast were grown on permissive (-WL) media, or selective (–WLH) media. Only yeast containing both pGADT7-NET2A and pGBKT7-PRK4 or pGBKT7-PRK5 were able to grow on selective media, indicating an interaction. Yeast containing pGADT7-NET2A and pGBKT7-PRK1, pGBKT7-PRK2, pGBKT7-PRK3 or pGBKT7-PRK6 were unable to grow on selective media, indicating no interaction between these proteins.

Fig. S4: NET2A-GFP is absent from transvacuolar cytoplasmic strands when co-expressed with PRK5-RFP in *N. benthamiana* leaf epidermal cells.

(a) cross-section of leaf epidermal cells expressing NET2A-GFP alone. Arrows indicate NET2A-GFP localising to transvacuolar cytoplasmic strands.

(b) cross-section of leaf epidermal cells co-expressing NET2A-GFP alongside PRK5-RFP. Scale bar: 10 µm.

Fig. S5: NET2A-GFP localises to actin filaments when co-expressed with PRK6-RFP in *N. benthamiana* leaf epidermal cells.

NET2A-GFP is not recruited to the plasma membrane. Scale bar: 10 µm

Fig. S6: NET2B-GFP is recruited to the plasma membrane by PRK4-RFP and PRK5-RFP in *N. benthamiana* leaf epidermal cells, but not by PRK6-RFP.

Scale bar: 10 µm

Table S1: Primers used in this study.

Table S2: NET2A does not interact with PRK1, PRK2, PRK3 or PRK6 in FRET-FLIM assays.

Each PRK was expressed as a GFP fusion in N. benthamiana either alone, or with NET2A-mCherry. The average fluorescence lifetimes of PRK1-GFP, PRK2-GFP, PRK3-GFP and PRK6-GFP were not significantly reduced by NET2A-mCherry, indicating no interaction between NET2A and each PRK. ± = standard deviation of mean values. ns = nanoseconds.

Table S3: NET2B interacts specifically with PRK4 and PRK5 in FRET-FLIM assays but not with PRK1, PRK2, PRK3 or PRK6.

NET2B was expressed alone, or with RFP-fluorophore fusions of each PRK. PRK4-RFP and PRK5-RFP were observed to reduce the fluorescence lifetime of NET2B-GFP, indicative of an interaction. The average fluorescence lifetime of NET2B-GFP was not decreased by PRK1-RFP, PRK2-mCherry, PRK3-RFP and PRK6-RFP indicating no interaction occurred. ± = standard deviation of mean values. ns = nanoseconds.

Video S1: NET2A-GFP Punctae Dynamics in Growing Pollen Tubes.

Figures

Fig. 1

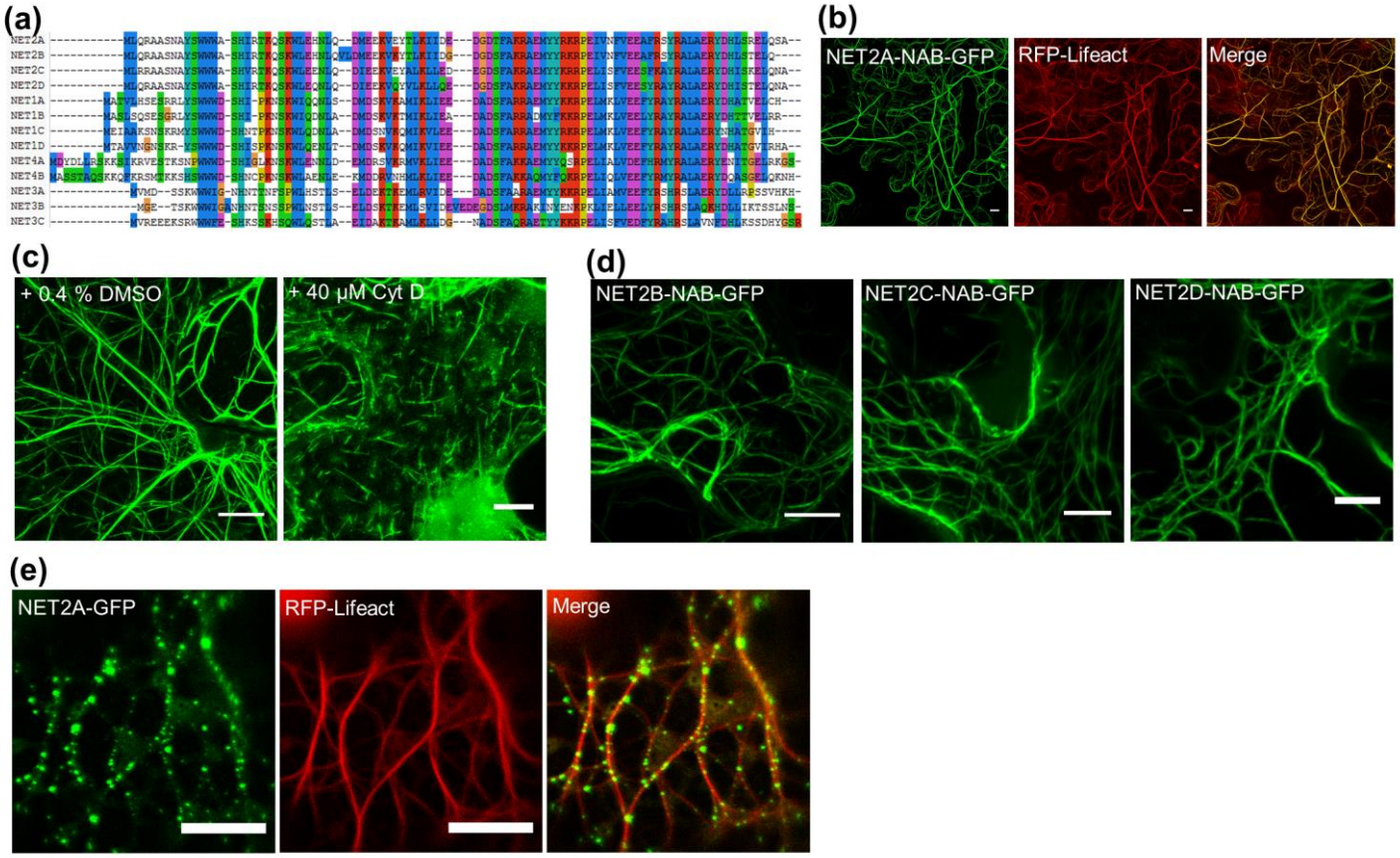

Fig. 2

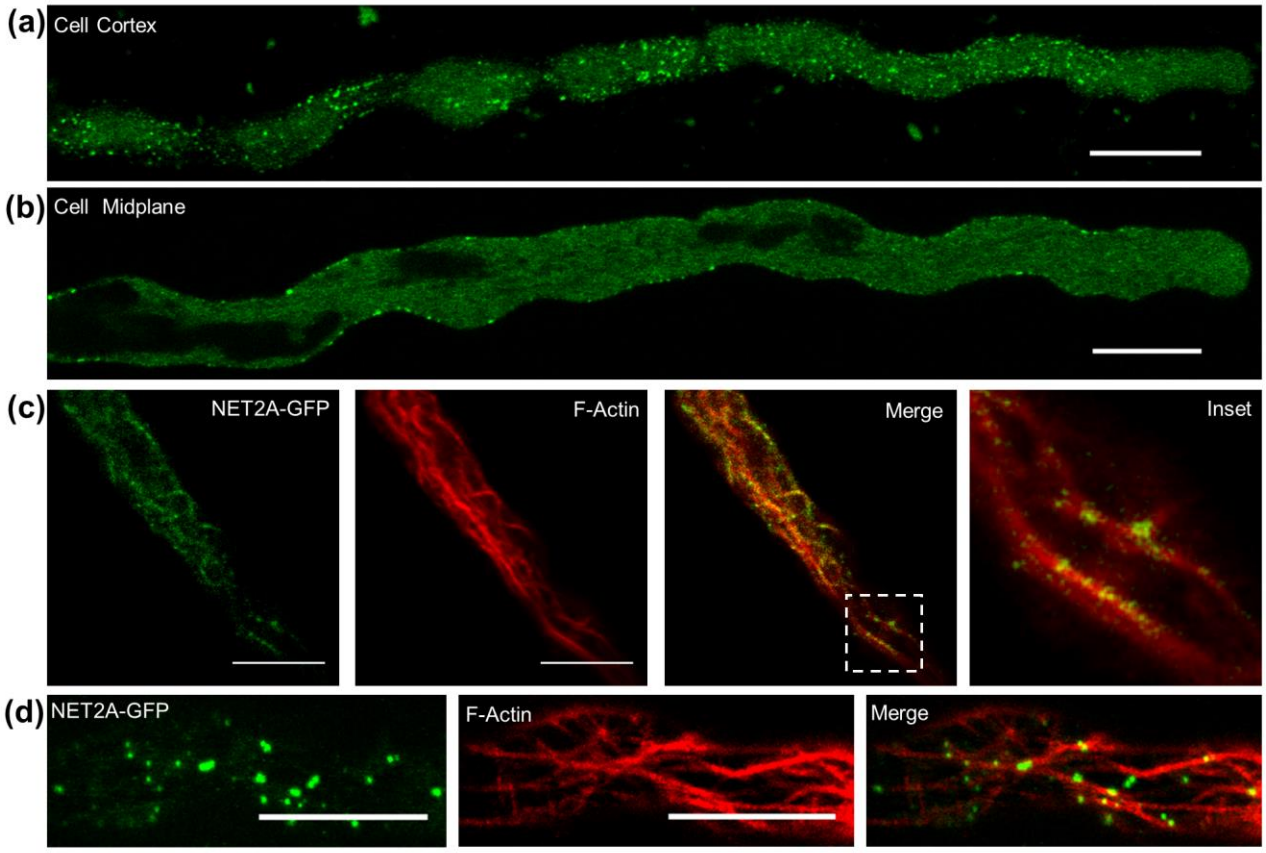
(a)
Cell Cortex
(b)
Cell Midplane
(c)
NET2A-GFP
F-Actin
Merge
Inset
(d)
NET2A-GFP
F-Actin
Merge

Fig. 3

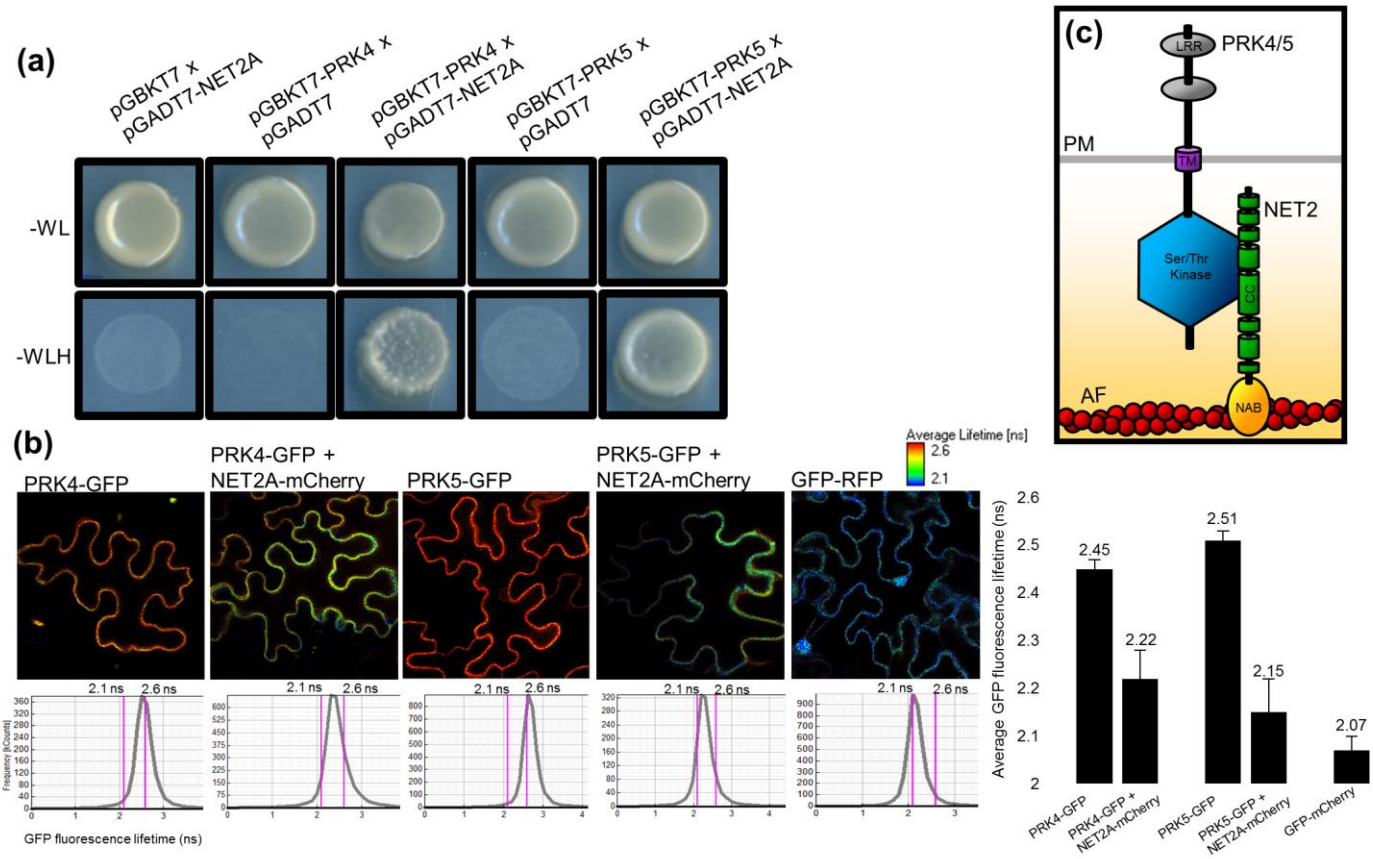
(a)
pGBKT7 x pGADT7-NET2A
pGBKT7-PRK4 x pGADT7
pGBKT7-PRK4 x pGADT7-NET2A
pGBKT7-PRK5 x pGADT7
pGBKT7-PRK5 x pGADT7-NET2A
-WL
-WLH
(b)
PRK4-GFP
PRK4-GFP + NET2A-mCherry
PRK5-GFP
PRK5-GFP + NET2A-mCherry
GFP-RFP
Average Lifetime [ns]
2.6
2.1
2.1 ns
2.6 ns
GFP fluorescence lifetime (ns)
Average GFP fluorescence lifetime (ns)
2.45
2.22
2.51
2.15
2.07
PRK4-GFP
PRK4-GFP + NET2A-mCherry
PRK5-GFP
PRK5-GFP + NET2A-mCherry
GFP-mCherry
(c)
LRR
PRK4/5
PM
TM
NET2
Ser/Thr Kinase
CC
AF
NAB

Fig. 4

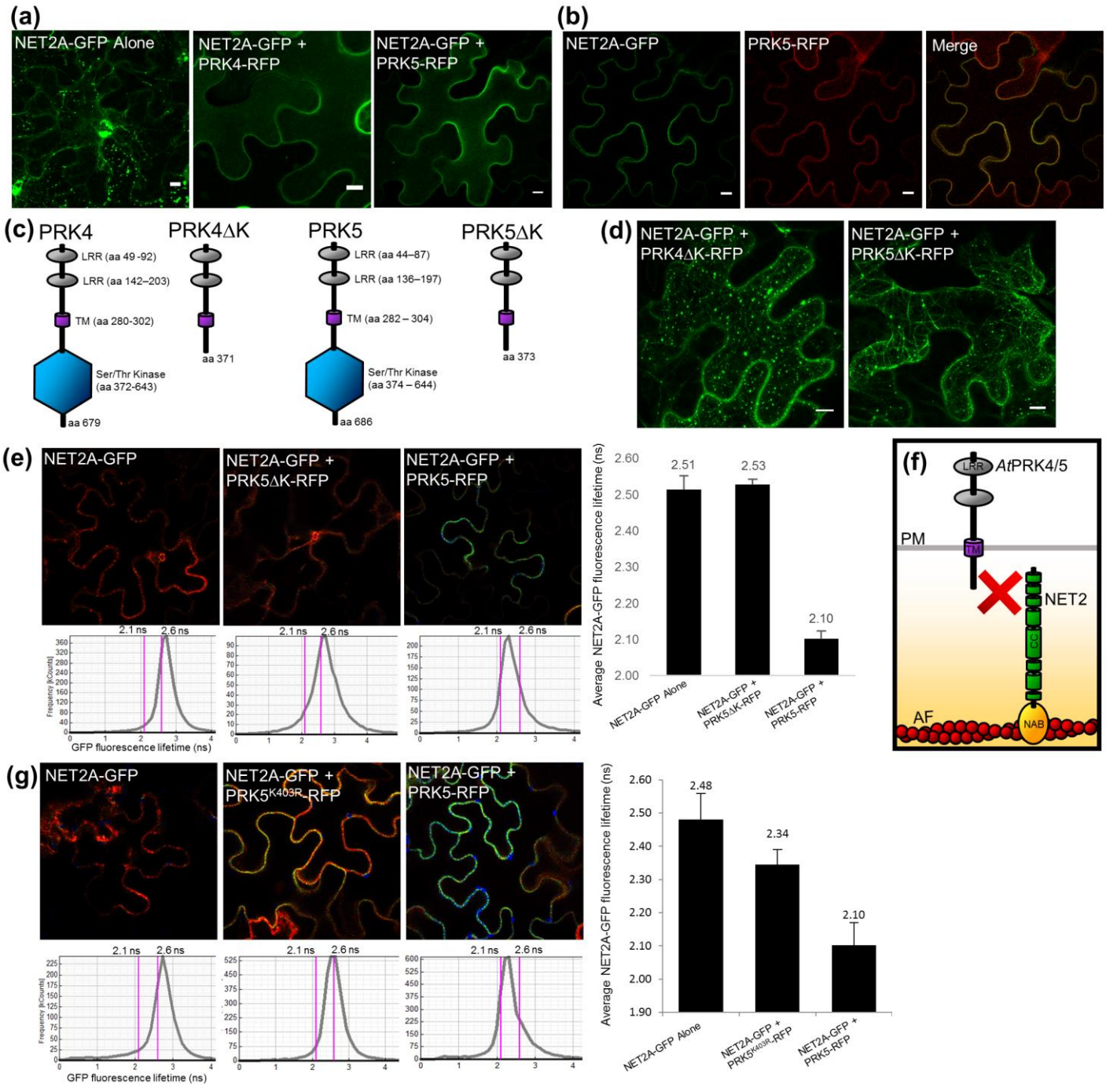
(a)
NET2A-GFP Alone
NET2A-GFP + PRK4-RFP
NET2A-GFP + PRK5-RFP
(b)
NET2A-GFP
PRK5-RFP
Merge
(c)
PRK4
LRR (aa 49-92)
LRR (aa 142–203)
TM (aa 280-302)
Ser/Thr Kinase (aa 372-643)
aa 679
PRK4ΔK
aa 371
PRK5
LRR (aa 44–87)
LRR (aa 136–197)
TM (aa 282 – 304)
Ser/Thr Kinase (aa 374 – 644)
aa 686
PRK5ΔK
aa 373
(d)
NET2A-GFP + PRK4ΔK-RFP
NET2A-GFP + PRK5ΔK-RFP
(e)
NET2A-GFP
NET2A-GFP + PRK5ΔK-RFP
NET2A-GFP + PRK5-RFP
2.1 ns
2.6 ns
Frequency [kCounts]
GFP fluorescence lifetime (ns)
Average NET2A-GFP fluorescence lifetime (ns)
2.51
2.53
2.10
NET2A-GFP Alone
NET2A-GFP + PRK5ΔK-RFP
NET2A-GFP + PRK5-RFP
(f)
LRR
AtPRK4/5
PM
TM
NET2
CC
AF
NAB
(g)
NET2A-GFP
NET2A-GFP + PRK5K403R-RFP
NET2A-GFP + PRK5-RFP
2.48
2.34
2.10
NET2A-GFP Alone
NET2A-GFP + PRK5K403R-RFP
NET2A-GFP + PRK5-RFP

Fig. 5

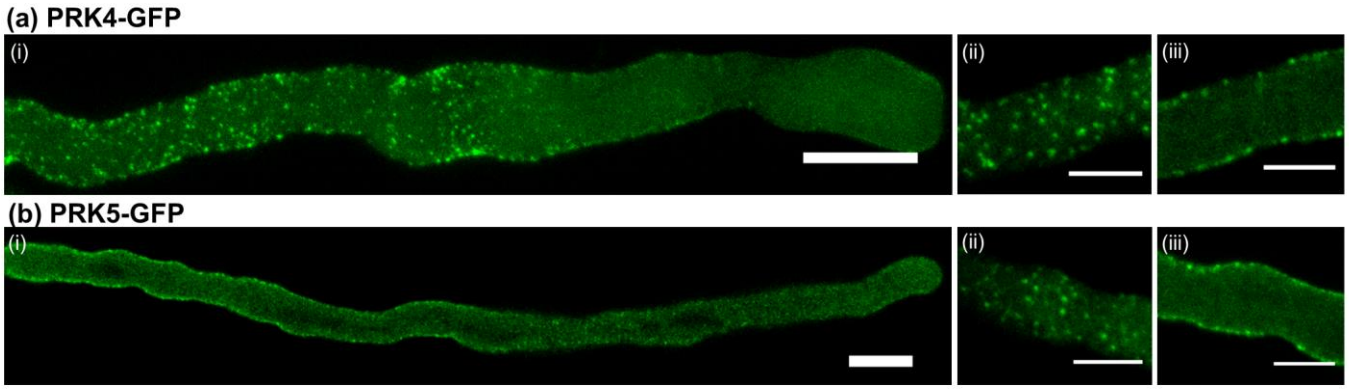

Fig. 6

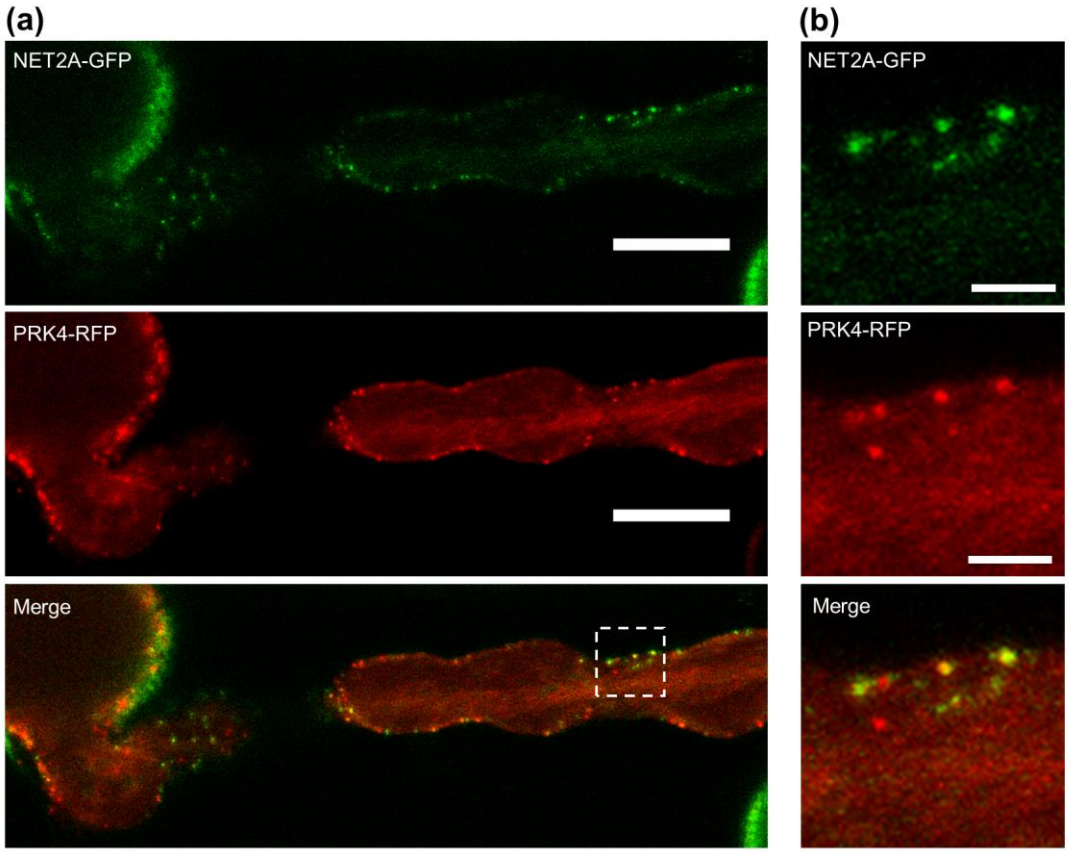

Supplemental Information

Fig. S1

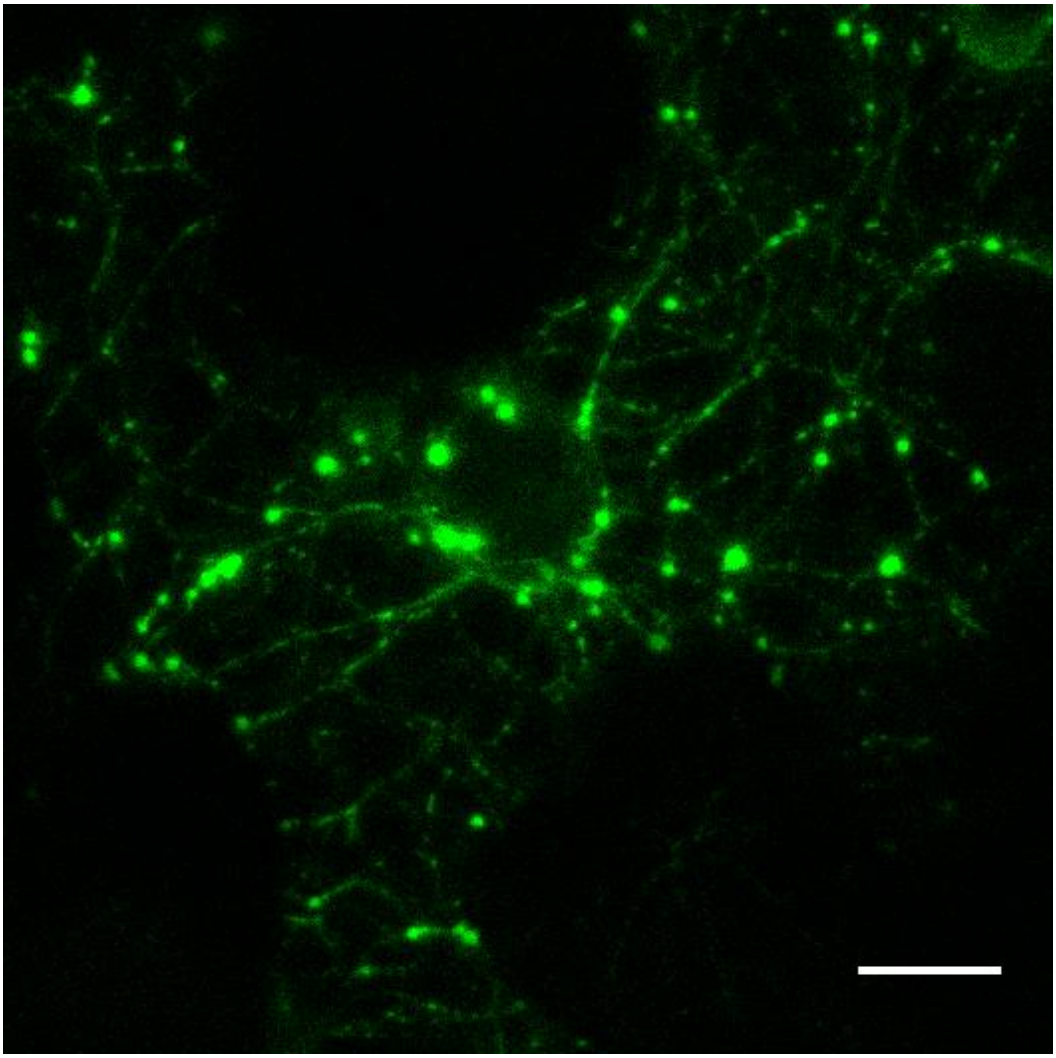

Fig. S2

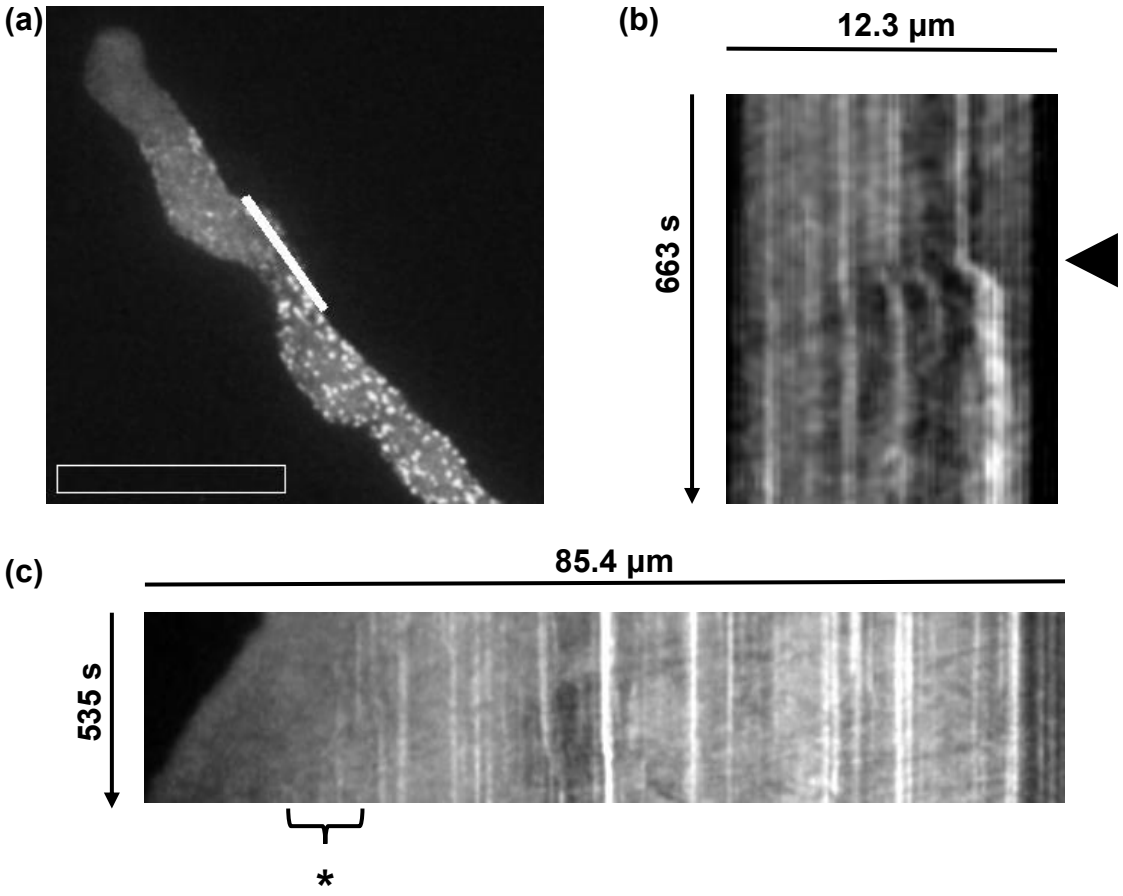

Fig. S3

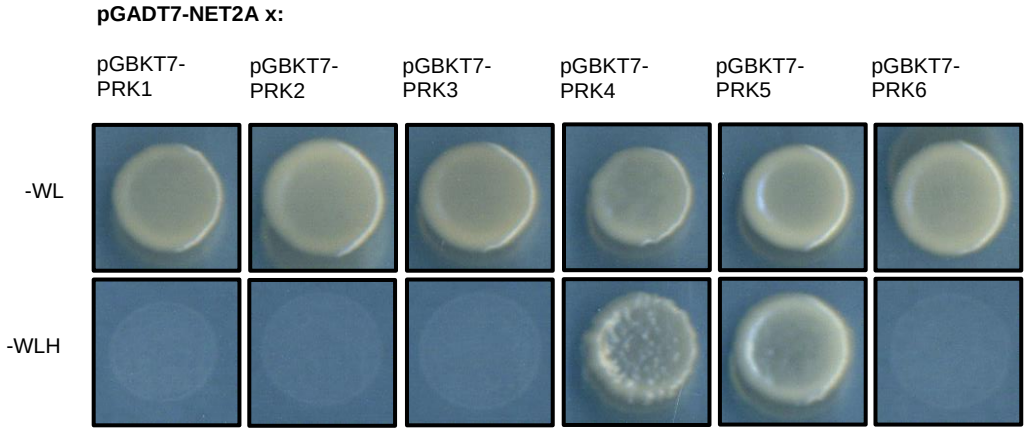
pGADT7-NET2A x:
pGBKT7-PRK1
pGBKT7-PRK2
pGBKT7-PRK3
pGBKT7-PRK4
pGBKT7-PRK5
pGBKT7-PRK6
-WL
-WLH

Fig. S4

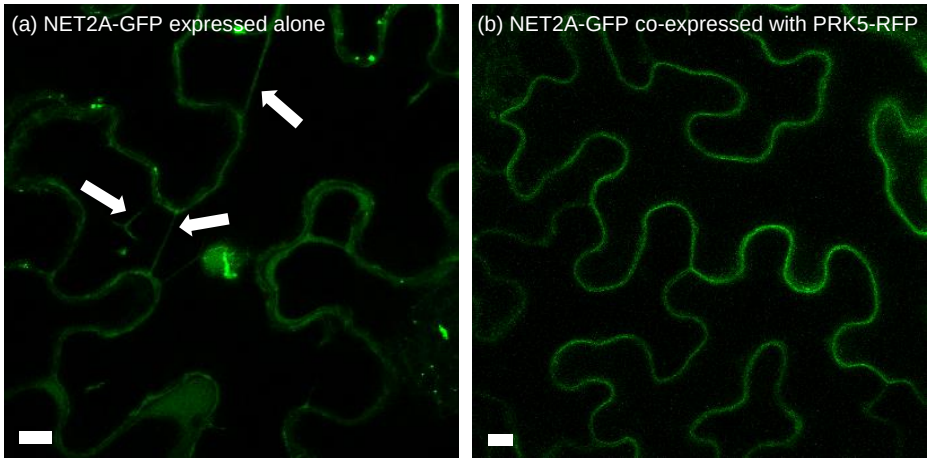
(a) NET2A-GFP expressed alone
(b) NET2A-GFP co-expressed with PRK5-RFP

Fig. S5

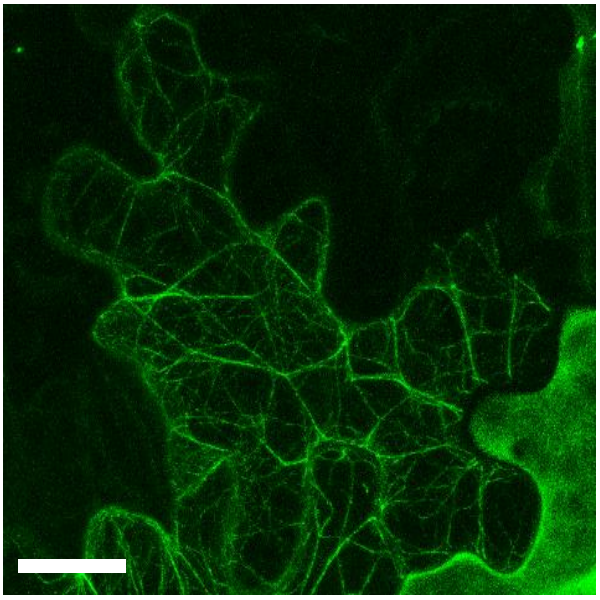

Fig. S6

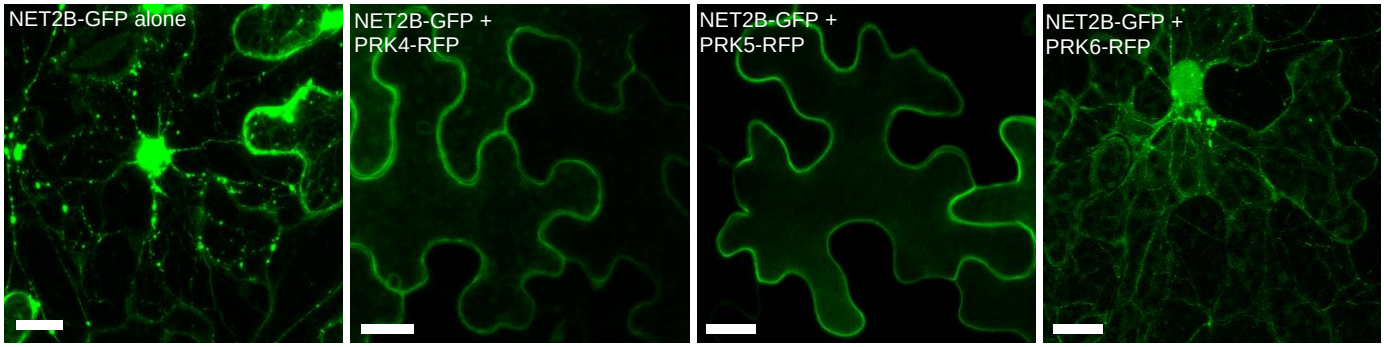
NET2B-GFP alone
NET2B-GFP +
PRK4-RFP
NET2B-GFP +
PRK5-RFP
NET2B-GFP +
PRK6-RFP

Table S1

Construct	Forward/Reverse	Primer Sequence 5'→3'
Full-length NET2A	F	GGGGACAAGTTTGTACAAAAAAGCAGGCTTCACCATGTTGCAGAGAGCAGCGAGC
	R	GGGGACCACTTTGTACAAGAAAGCTGGGTCTTCAGGGAGCTTCCCAGGTG
Full-length NET2B	F	GGGGACAAGTTTGTACAAAAAAGCAGGCTTCACCATGTTGCAGAGAGCAGCGAGC
	R	GGGGACCACTTTGTACAAGAAAGCTGGGTCGCTTCTTTTGACATATTCAGG
Full-length PRK1	F	GGGGACAAGTTTGTACAAAAAAGCAGGCTTCACCATGCCTCCCATGCAGGCG
	R	GGGGACCACTTTGTACAAGAAAGCTGGGTCTGCAAAGCTGATACTCTC
Full-length PRK2	F	GGGGACAAGTTTGTACAAAAAAGCAGGCTTCACCATGGAATCCAAATGTCTCATGTTCG
	R	GGGGACCACTTTGTACAAGAAAGCTGGGTCTGACAAGTTAATTCCCTCAC
Full-length PRK3	F	GGGGACAAGTTTGTACAAAAAAGCAGGCTTCACCATGACTGCTGTTCTATTT
	R	GGGGACCACTTTGTACAAGAAAGCTGGGTCAAGTGTTACTCGTTCTAT
Full-length PRK4	F	GGGGACAAGTTTGTACAAAAAAGCAGGCTTCACCATGCTAACTTGGGAGACC
	R	GGGGACCACTTTGTACAAGAAAGCTGGGTCTCGATTCATGGCGAAACC
Full-length PRK5	F	GGGGACAAGTTTGTACAAAAAAGCAGGCTTCACCATGCGCAATTGGGAGGAC
	R	GGGGACCACTTTGTACAAGAAAGCTGGGTCTCGATTCATCGAGAAACCA
Full-length PRK6	F	GGGGACAAGTTTGTACAAAAAAGCAGGCTTCACCATGGCTGCTGCTGTTCTG
	R	GGGGACCACTTTGTACAAGAAAGCTGGGTCAGTTTTTACTTGTTCTATCCTTCTA
NET2B-NAB (NET2B$^{1-93}$)	F	GGGGACAAGTTTGTACAAAAAAGCAGGCTTCACCATGTTGCAGAGAGCAGCGAGC
	R	GGGGACCACTTTGTACAAGAAAGCTGGGTCTTGAAGTTCTGTGGACAAATGATC
NET2C-NAB (NET2C$^{1-93}$)	F	GGGGACAAGTTTGTACAAAAAAGCAGGCTTCACCATGCTACGAAGAGCTGCGAGC
	R	GGGGACCACTTTGTACAAGAAAGCTGGGTCGGCGTTTTGAAGCTCTTTAGAG
NET2D-NAB (NET2D$^{1-93}$)	F	GGGGACAAGTTTGTACAAAAAAGCAGGCTTCACCATGCTGCAACGAGCTGCGAGTAATG
	R	GGGGACCACTTTGTACAAGAAAGCTGGGTCAGCATTTTGAAGCTCTGTAG
PRK4ΔK (PRK4$^{1-374}$)	F	GGGGACAAGTTTGTACAAAAAAGCAGGCTTCACCATGCTAACTTGGGAGACC
	R	GGGGACCACTTTGTACAAGAAAGCTGGGTCAGAGGCTCTAAGAAGATCTTGAAGG
PRK5ΔK (PRK5$^{1-376}$)	F	GGGGACAAGTTTGTACAAAAAAGCAGGCTTCACCATGCGCAATTGGGAGGAC
	R	GGGGACCACTTTGTACAAGAAAGCTGGGTCAGCTCTCAAAAGATCTTGAAGATCG
5'AscI-mCherry-*3'BstB*I	F	CTTGGCGCGCCATGGTGAGCAAGGGCGAGGAGGATAA
	R	TCTTTCGAATTACTTGTACAGCTCGTCCATGCC
5'SacI-pLAT52-*3'SpeI*	F	TCAGGAGCTCTTGAGGAATGATCGATTCTGG
	R	CCATACTAGTGAATTTTTTTTTTGGTGTGTG
PRK5^{K403R}	F	GTGGACAAACATTGGTTGTGAGGAGGTATAAACATATGAACAATG
	R	CATTGTTCATATGTTTATACCTCCTCACAACCAATGTTTGTCCAC
NET2A Y2H	F	GGGGACAAGTTTGTACAAAAAAGCAGGCTTCACCATGTTGCAGAGAGCAGCGAGC
	R	GGGGACCACTTTGTACAAGAAAGCTGGGTCTTATTCAGGGAGCTTCCCAGGTG
PRK1 Y2H	F	GGGGACAAGTTTGTACAAAAAAGCAGGCTTCACCATGCCTCCCATGCAGGCG
	R	GGGGACCACTTTGTACAAGAAAGCTGGGTCTGCAAAGCTGATACTCTC

PRK2 Y2H	F	GGGGACAAGTTTGTACAAAAAAGCAGGCTTCACCATGGAATCCAAATGTCTCATGTTCG
	R	GGGGACCACTTTGTACAAGAAAGCTGGGTCTGACAAGTTAATTCCCTCAC
PRK3 Y2H	F	GGGGACAAGTTTGTACAAAAAAGCAGGCTTCACCATGACTGCTGTTCTATTT
	R	GGGGACCACTTTGTACAAGAAAGCTGGGTCAAGTGTTACTCGTTCTAT
PRK4 Y2H	F	GGGGACAAGTTTGTACAAAAAAGCAGGCTTCACCATGCTAACTTGGGAGACC
	R	GGGGACCACTTTGTACAAGAAAGCTGGGTCTCGATTCATGGCGAAACC
PRK5 Y2H	F	GGGGACAAGTTTGTACAAAAAAGCAGGCTTCACCATGCGCAATTGGGAGGAC
	R	GGGGACCACTTTGTACAAGAAAGCTGGGTCTCGATTCATCGAGAAACCA
PRK6 Y2H	F	GGGGACAAGTTTGTACAAAAAAGCAGGCTTCACCATGGCTGCTGCTGTTCTG
	R	GGGGACCACTTTGTACAAGAAAGCTGGGTCAGTTTTTACTTGTTCTATCCTTCTA

Table S2

	Mean Donor GFP Fluorescence Lifetime			
Donor Construct	Expressed without NET2A-mCherry	n	Co-expressed with NET2A-mCherry	n
PRK1-GFP	2.50 ± 0.03 ns	6	2.49 ± 0.02 ns	6
PRK2-GFP	2.57 ± 0.02 ns	10	2.54 ± 0.03 ns	10
PRK3-GFP	2.47 ± 0.02 ns	10	2.52 ± 0.02 ns	10
PRK6-GFP	2.43 ± 0.04 ns	10	2.43 ± 0.07 ns	10
GFP-mCherry	2.07 ± 0.03 ns			12

Table S3

Constructs Expressed	Mean GFP Fluorescence Lifetime (ns)	n
NET2B-GFP	2.50 ± 0.04	10
NET2B-GFP + PRK1-RFP	2.46 ± 0.03	10
NET2B-GFP + PRK2-mCherry	2.50 ± 0.04	10
NET2B-GFP + PRK3-RFP	2.48 ± 0.02	10
NET2B-GFP + PRK4-RFP	2.22 ± 0.14	10
NET2B-GFP + PRK5-RFP	2.14 ± 0.09	10
NET2B-GFP + PRK6-RFP	2.47 ± 0.06	10
GFP-RFP	1.99 ± 0.04	5
GFP-mCherry	2.03 ± 0.05	5